Journal of Photochemistry & Photobiology, A: Chemistry 428 (2022) 113869

Contents lists available at ScienceDirect

Journal of Photochemistry & Photobiology, A: Chemistry

journal homepage: www.elsevier.com/locate/jphotochem

# Azobenzene photoisomerization dynamics: Revealing the key degrees of freedom and the long timescale of the trans-to-cis process

Anna Kristina Schnack-Petersen [a,*], Mátyás Pápai [a,b], Klaus Braagaard Møller [a]

[a] Department of Chemistry,Technical University of Denmark, DK-2800 Kongens Lyngby, Denmark
[b] Wigner Research Centre for Physics, P.O. Box 49, H-1525 Budapest, Hungary

ARTICLE INFO

*Keywords:*
SHARC
Surface hopping
Azobenzene
Molecular dynamics
TDDFT

ABSTRACT

The photoisomerization reaction of azobenzene in both directions have been investigated with a density functional theory based approach using the surface hopping procedure with forced jumps. While the cis-to-trans isomerization was found to be a stepwise reaction along the CNNC dihedral angle, the trans-to-cis isomerization was observed to be one smooth step. The further unbiased full-dimensional analysis of the cis-to-trans isomerization revealed that, while the CNNC dihedral angle is an important degree of freedom for describing the reaction, it is insufficient for describing all of the dynamics. For a fuller picture two coupled modes must be considered. The trans-to-cis isomerization on the other hand was found to be well described along only the CNNC dihedral angle, and its longer timescale could be ascribed to the slow oscillations of this degree of freedom rather than a potential energy barrier in the excited state. The timescales observed in this study was found to be in good agreement with experiment, and thus this work provides insights into the interpretation of experimental observations. Finally, investigations of the structures of the CIs for both reactive and non-reactive trajectories showed a heavy functional dependency.

## 1. Introduction

Ever since the discovery of the photo-induced isomerization process of azobenzene in 1937 by Hartly [1], the molecule and its derivatives have been studied widely both experimentally [2] and theoretically [3–12]. The appeal of azobenzene derivatives stems from the many possible applications of the molecules [13]. This class of molecules is widely considered promising for applications in optical data storage and information transfer [14–20] and generally as good photoswitches [15,21,22], not to mention their applicational interest for photomodulable surfaces [23–25] and molecular machines and motors [26–29].

Despite the efforts to uncover the dynamics of azobenzene, the photoisomerization reaction is still not fully understood and both theoretical [3,4,10,20,22,30–35] and experimental [25,36] studies continue to be published. It remains unclear why the trans-to-cis isomerization happens on a significantly longer timescale than the cis-to-trans isomerization. A possible reason could be an energy barrier on the potential energy surface (PES) of the trans-to-cis isomerization, however not all theoretical studies have found such a barrier [2]. Also, the dynamics after the transition to the ground state is not clear, e.g. it is not known if the isomerization process happens stepwise or not. While the structure of the two isomers are characterized well by experiments [2] the reaction path is less well defined. Many theoretical and experimental studies agree that the cis-to-trans isomerization follows a rotational path [2,3,6], however studies of the trans-to-cis isomerization do not agree whether a rotation or inversion pathway is dominant for the non-reactive pathway [2,3,5,7,30,32,37]. In addition, a twist mechanism has also been suggested for both isomerization reactions [9–12]. In fact, while studies suggest two distinguishable conical intersections (CIs) – a rotated and a planar – they seem to disagree about the importance of the planar CI [5,8,37]. Finally, the important degrees of freedom (DOFs) have not been studied thoroughly as it is generally acknowledged that the degree of freedom of main importance is the CNNC dihedral angle. While a few studies [8,10,12,30,31] suggested that one should consider other degrees of freedom, the main conclusion of a recent extensive study of the trans-to-cis isomerization by Tavadze et al. [30] was, that the trans-to-cis isomerization process was heavily dominated by the change in the CNNC dihedral angle, justifying that it is usually the only degree of freedom considered when investigating the PES of the reaction [3,5,6,30]. Studies focused on the cis-to-trans isomerization also acknowledged the need to consider more degrees of freedom [9,10,38]. Here however, a few degrees of freedom were chosen a priori for the investigations, and were found to give a reasonable description of the reaction.

* Corresponding author.
*E-mail addresses:* akrsc@kemi.dtu.dk (A.K. Schnack-Petersen), kbmo@kemi.dtu.dk (K.B. Møller).

https://doi.org/10.1016/j.jphotochem.2022.113869
Received 17 November 2021; Received in revised form 21 January 2022; Accepted 17 February 2022
Available online 26 February 2022
1010-6030/© 2022 The Authors. Published by Elsevier B.V. This is an open access article under the CC BY license (http://creativecommons.org/licenses/by/4.0/).

The dynamics of azobenzene have been studied with a range of theoretical methods. The dynamics have been simulated with e.g. surface hopping [7,10], while the electronic structure calculations have been performed with e.g. complete active space self consistent field (CASSCF) [6,37], complete active space 2nd order perturbation theory (CASPT2) [5] and (time-dependent) density functional theory ((TD-)DFT) [3,4,22]. DFT has proven a very powerful method with wide applications [39]. It is widely applicable even to large systems [39] and yields results in good agreement with experiment when calculating electronic excitation energies [39–41] in particular, but also when computing other properties [39,42]. Unfortunately, TD-DFT often gives questionable results close to CIs between the ground and first excited singlet state, as the ground state is described by a single Slater determinant. This leads to various problems, e.g. the rapid variation of the potential energy of response states in this area [43] and an artificial double cone structure of the CI [3]. It has previously been seen [44,45] that by utilizing surface hopping for the dynamics [46] and in addition invoking forced hops to the ground state, when the potential energy gap between states decrease below a certain threshold, this problem can be circumvented. In both previous studies a potential energy threshold of 0.15 eV has been used [44,45]. Thus, all trajectories have been forced to jump to a new state if the potential energy difference between the current state of the trajectory and the ground state (GS) drops to this threshold or below. Following these forced jumps, trajectories are no longer allowed to jump, but moves on the GS-PES for the remainder of the simulation. In the current study we employ the same strategy and value for the potential energy threshold as in the previous studies [44,45].

It should be observed that when employing the forced jump approach, one *will* underestimate relaxation lifetimes. In addition, the geometry at which a trajectory jumps from the excited state (ES) to the GS will influence whether or not isomerization occurs. Thus, the probability of isomerization, and hence the quantum yield (QY), is affected by fixing an energy gap to force jumps.

By computing the PESs along the CNNC dihedral angle several interesting observations can be made albeit a deeper understanding of the dynamics naturally requires further investigations. Considering the relaxed PESs (for the BHHLYP functional) shown in Fig. 1a, it is observed that while the path is downhill from the cis-isomer in the $S_1$ ES all the way to the CI, the path from the trans-isomer is much flatter. For the latter a slight slope downhill is observed from approximately 180° to approximately 105°, while the slope is slightly uphill on the last stretch up to the CI geometry, which might indicate a potential energy barrier that could slow down the reaction. These PESs are found to closely resemble those obtained by Pederzoli et al. [6] using SA3-CASSCF(10,8), those obtained by Hutcheson et al. [47] using coupled cluster (CC3), the ones by Yu et al. [32] using both CASPT2 and TDDFT, as well as the ones obtained by Ye et al. [4] using several different DFT/TDDFT methods.

Investigating Fig. 1a further, one can observe that when forcing the jump at 0.15 eV, the jump from trans-to-cis is expected to happen when the dihedral angle reaches a value of approximately 105°, which is nicely beyond the grey area in which the PESs plotted here cannot be expected to provide a good representation of the actual PESs and where problems in the calculations might arise from being too close to the CI. Indeed, no such convergence problems arise for the trans-to-cis isomerization. It should also be noted that the jump thus occurs before the slight upwards slope towards the CI is encountered, and thus this feature of the ES-PES is not expected to significantly influence the investigated dynamics in this study. Considering the cis-to-trans isomerization path, it is found that the jumps are expected to happen when the dihedral angle reaches approximately 85°, and thus rather close to the grey area and the CI compared to the trans-to-cis isomerization. Hence, these results might be expected to suffer somewhat from the close proximity to the CI, and indeed for some trajectories convergence becomes more cumbersome in this region (see Supporting Information (SI), section 2.1). Another interesting point to note from Fig. 1a is that the slope of the ES-PES appears to be steeper on the cis-isomer side compared to the trans-isomer side of the CI. Thus, once a trajectory reaches the CI, we would expect that it has picked up more speed and is therefore more likely to continue in the forward direction after the jump coming from the cis-isomer side than coming from the trans-isomer side. Hence, the QY of the cis-to-trans isomerization is expected to be significantly larger than the QY from the trans-to-cis isomerization, and that is indeed what is observed both here, in other calculations [3] and in experiment [2].

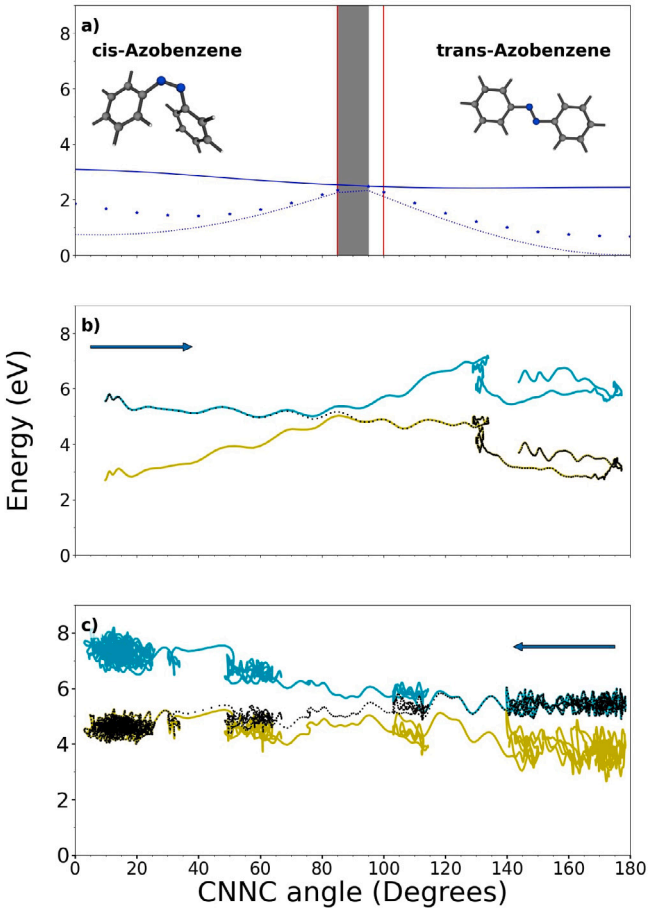


**Fig. 1.** (a) Calculated PESs along CNNC dihedral angle for $S_0$ using relaxed GS structures (dashed), $S_1$ using relaxed ES structures (solid) and $S_0$ calculated from relaxed ES structures (stars). Optimized structures could not be obtained in the grey area due to a too close proximity to the CI. Vertical red lines show the calculated points where the potential energy gap between $S_1$ and $S_0$ (calculated from ES structures) fall below 0.15 eV, and hence where our trajectories are not expected to go due to the chosen potential energy gap. The trans-isomer is shown in the inset on the right, while the cis-isomer is shown in the inset on the left. (b) Average electronic energy evolution of $S_0$ (green) and $S_1$ (cyan), and average potential energy evolution of the actual trajectory energy (black dots) from reactive cis-to-trans isomerization trajectories. (c) Average electronic energy evolution of $S_0$ (green) and $S_1$ (cyan), and average potential energy evolution of the actual trajectory energy (black dots) from reactive trans-to-cis isomerization trajectories. The arrows in (b) and (c) show the direction of reaction.

At each timestep, the average CNNC dihedral angle as well as the average electronic energy for both GS and ES can be determined from the reactive trajectories. These average electronic energies, as well as the average potential energy of the reactive trajectories, are shown in Fig. 1b and c as a function of the corresponding average CNNC dihedral angle.

While the ES and GS electronic energies will of course be simple averages throughout the entire range, the average of the potential energy of the actual trajectory cannot be considered as such in the

region where the jumps to the ground state occur. Here, the average potential energy will in fact also be an average of the GS and ES energies as not all trajectories jump at the same time and dihedral angle. We observe that this region is significantly larger for the trans-to-cis isomerization in Fig. 1c, indicating a larger spread in the jump angles for this reaction, resulting in a larger spread of the jump times, as can be observed comparing Figs. 7 and 16.

Comparing the calculated PESs in Fig. 1a to the actual simulated evolution of the average potential energy (including zero point vibrational energy (ZPVE)) as a function of dihedral angle for reactive cis-to-trans trajectories (Fig. 1b), it is observed that the simulation seems to qualitatively follow the ES-PES towards the CI. After the jump, the potential energy is roughly constant until the CNNC angle reaches 130°, where it makes a significant drop and then qualitatively follows the GS-PES towards the trans-isomer. This very abrupt drop in energy at 130° is particularly interesting, as it indicates that other DOFs than the CNNC dihedral angle might be necessary to consider in order to fully describe the reaction.

Considering also the average of the simulated reactive trans-to-cis trajectories (Fig. 1c), one can recognize that this does indeed also qualitatively follow the calculated shape of the PESs albeit oscillations occur in the potential energy due to motion in other degrees of freedom, e.g. the CNN angles. The oscillations in the potential energy observed are noted to be larger on the cis-side in accordance with the molecule being in possession of excess kinetic energy after the jump. This behaviour is also observed for the cis-to-trans trajectory in Fig. 1b, where more oscillations are seen on the trans-side. Observe also that the ES electronic energy in Fig. 1b and c after the point of jump will never be reached as the trajectories here move on the GS, and thus these are not discussed.

In this study, we shed light on the origin of the slow trans-to-cis isomerization, showing that it is not a result of a large potential energy barrier in the ES, but rather of the reaction following slow oscillations in the CNNC dihedral angle. Furthermore, we show how the cis-to-trans isomerization happens as a result of motion along at least two degrees of freedom. Finally, we add to the discussion of the role of the planar CI, which appears inaccessible when applying one DFT functional, while it appears very important for the non-reactive trans-to-trans pathway, when another functional is applied.

## 2. Computational methods

The non-adiabatic dynamics simulations [48] were run with the SHARC-2.1.1 program package [49] and the required quantum chemistry TD-DFT calculations were performed by the ORCA-4.2.0 program package [50,51].

For the surface hopping [46], a timestep of 0.5 fs was employed and a potential energy gap of 0.15 eV was specified for forcing the trajectories to jump from one surface to another. In order to ascertain that the chosen potential energy gap gives a sufficiently good description of the molecular dynamics, another smaller potential energy gap was considered. Here, it was found that the behaviour of the trajectories were the same, except for a larger QY for the smaller potential energy gap. This however, is likely to be caused by the closer proximity to the CI, where the calculations become unreliable, and thus the chosen potential energy gap was deemed the most suitable. For more information see section 2.1 of the SI.

A recent study of the functional and basis set sensitivity was carried out for the cis-to-trans isomerization reaction of Azobenzene by Ye et al. [4] and their results as well as our subsequent study of the PESs, have guided our choice of basis set and functional. Thus we have utilized the BHandHLYP (BHHLYP) functional and cc-pVDZ basis set in the present study. For more details see section 1 of the SI.

For both the cis-to-trans and trans-to-cis isomerization 1000 initial conditions were prepared based on a Wigner distribution at zero kelvin determined by SHARC python scripts. The 3 lowest lying singlet states ($S_0$, $S_1$ and $S_2$) were considered in the calculations. Based on calculated excitation energies to the $S_1$ state from the two isomers excitation energies, an upper bound of the excitation energy of 3.0 eV was chosen for the cis-to-trans isomerization to ensure starting the trajectories in the $S_1$ state. This resulted in 37 trajectories to be simulated for 250 fs in accordance with the experimental lifetime. Likewise, an upper bound of the excitation energy of 4.0 eV was chosen for the trans-to-cis isomerization, giving 38 trajectories to be simulated for up to 2.0 ps corresponding to the longer lifetime of this reaction. Observe that the $S_2$ state was included in the simulation to allow for more flexibility, however in the simulations carried out for this study it was found to play no role in the reaction. Additional details can be found in section 1 of the SI.

The ORCA-4.2.0 program package has been used both for on-the-fly PES calculations needed by SHARC, as well as for the static PESs of the isomerization reaction along one or two DOFs. Observe that the CI structures were only possible to obtain when using the SHARC program interface [52], where gradients and energies (both potential and kinetic) were calculated by ORCA.

Visualization of the trajectories was done with the VMD-1.9.1-program [53] and OVITO [54], while vizualization of the normal modes was done using molden [55].

As a way of verifying that the results obtained at the current level of theory are sound and that the simulated molecular dynamics are qualitatively accurate, we investigate the QY and timescale of the reaction. The timescale obtained using forced jumps might be expected to be too short, and also the QYs might be more uncertain. As long as a reasonable agreement with previous studies can be obtained however, the overall dynamics is expected to be unchanged. Due to the procedure of forcing the jump combined with previous studies indicating non-exponential dynamics [3,6], the lifetimes as such are not reported, but rather the lag times, i.e. the average time before a jump to the ground state is observed as also seen in Pápai et al. [45]. These are considered only for the reactive trajectories, since the point of interest in this study is the isomerization. The reactive trajectories are, thus, defined as trajectories that end up in the ground state of the isomer different from the one in which they began. Likewise, unreactive trajectories are those that end up in the ground state of the same isomer as the one in which they began. The QYs are reported as the percentage of reactive trajectories.

## 3. Conical intersections

In addition to investigating the one dimensional PESs along the CNNC dihedral angle it can also be useful to study some of the key structures of the reaction namely the cis- and trans-isomer GS structures as well as the CI structures. In this study, using the BHHLYP functional, no planar CI could be obtained, and all CI geometry optimizations of the jumping geometries of reactive as well as non-reactive trajectories for both the cis-to-trans and trans-to-cis isomerization resulted in the same rotated CI (see Fig. 2) in agreement with previous results [8,37] and as also indicated by the reported jumping geometries of Yue et al. [3], who found the dihedral angle at the time of the jump for the trans-to-cis isomerization to be around 120°. This contrasts however to the findings by Casellas et al. [5] and Yu et al. [32], who found also a planar CI, which was suggested to play a role for the non-reactive trans-to-cis trajectories. In addition this planar CI was also found to be of importance when employing the B3LYP functional rather than the BHHLYP functional (see SI, section 3.4). The CI determined in this study is in good agreement with the reported rotated CI found in other studies [3,5,6].

The average structure of the rotated CI is in addition presented in Table 1 along with the structures of the GS of the two isomers for some key geometrical parameters. From this table, we observe that while the CNNC dihedral angle and to some extent also the CNN angles and CN bond lengths change significantly upon going from the relaxed GS

**Fig. 2.** Structure of the rotated (left) and planar (right) CI. The former structure is from one of the reactive trans-to-cis trajectories, while the latter is from a non-reactive trans-to-cis trajectory run with B3LYP (see SI section 3.4), as the planar CI was not observable using BHHLYP. As can be seen from the SI all optimized CI structures from both reactive and non-reactive trajectories are very similar using the BHHLYP functional, and thus the shown rotated structure can be assumed representative.

**Table 1**
Geometry of GS cis and trans geometries as well as average optimized CI from jumping geometries of all trajectories for which the rotated CI is obtained.

| Parameter | GS cis | | Avg. rotated CI | GS trans | |
|---|---|---|---|---|---|
| | Theory | Exp. [56] | Theory | Theory | Exp. [57] |
| Dihedral angle ($C_1N_1N_2C_7$) | 7.538° | 8.0° | 92.371° | 179.998° | 180.0°[a] |
| Angle ($C_4C_1N_1$) | 173.943° | – | 177.689° | 175.449° | – |
| Angle ($C_{10}C_7N_2$) | 173.943° | – | 177.677° | 175.450° | – |
| Angle ($C_1N_1N_2$) | 123.712° | 121.9° | 119.613° | 115.179° | 114.1° |
| Angle ($C_7N_2N_1$) | 123.712° | 121.9° | 137.142° | 115.179° | 114.1° |
| Bond length ($N_1N_2$) | 1.229 Å | 1.253 Å | 1.247 Å | 1.235 Å | 1.259 Å |
| Bond length ($C_1N_1$) | 1.429 Å | 1.449 Å | 1.393 Å | 1.414 Å | 1.428 Å |
| Bond length ($C_7N_2$) | 1.429 Å | 1.449 Å | 1.347 Å | 1.414 Å | 1.428 Å |

[a]Coplanarity of $C_1N_1N_2C_7$ assumed.

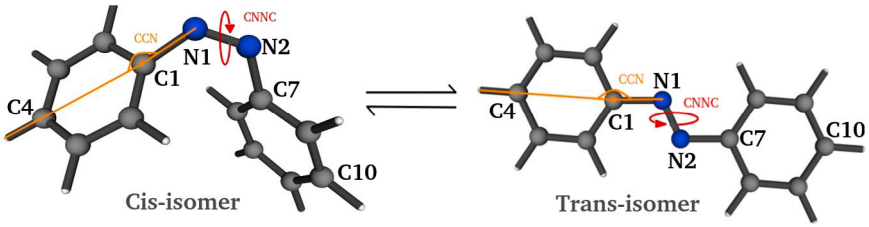


**Fig. 3.** The CNNC dihedral angle (red) and CCN angle (orange) marked on the structure of both the cis- (left) and trans-isomer (right). Relevant atom labels are depicted in black.

structure of either isomer to the CI structure, the remaining degrees of freedom change only very little, and we would not expect these to play a major role in the reaction. However, as we shall see, this is not the case for the CCN angle between $N$ of the azo-bond and the nearest and para C's of the benzene ring (See Fig. 3).

Considering now the jumping geometries we investigate Fig. 4. Firstly, it is noted that the predictions made about the CNNC dihedral angle at the time of jump based on Fig. 1a is in good agreement with the results observed in Fig. 4. Here, it is evident that only very few cis-to-trans trajectories and no trans-to-cis trajectories enter the grey area of Fig. 1a. It is observed that while most of the trajectories do jump at CNNC dihedral angles close to that of the rotated CI, a few of the non-reactive trans-to-cis trajectories appear to jump at a significantly larger dihedral angle. This might be indicative of these trajectories moving towards the predicted planar CI. In the study by Yu et al. [37] it was found that 45.4% of the non-reactive trajectories do go through a planar CI (see Fig. 2), with a dihedral angle of 180° [37]. This other planar CI has also been reported by other studies [3,5], however it was remarked by Casellas et al. [5] that the path towards the rotated CI would be preferred for systems without constrained rotation. By attempting to optimize a CI structure of a geometry very close to the reported planar CI, the rotated CI was once again obtained (see SI, Table 13).

Also note from Fig. 4 that the cis-to-trans trajectories jump at a significantly lower CCN angle than the trans-to-cis trajectories, indicating that this degree of freedom plays a role in the cis-to-trans isomerization.

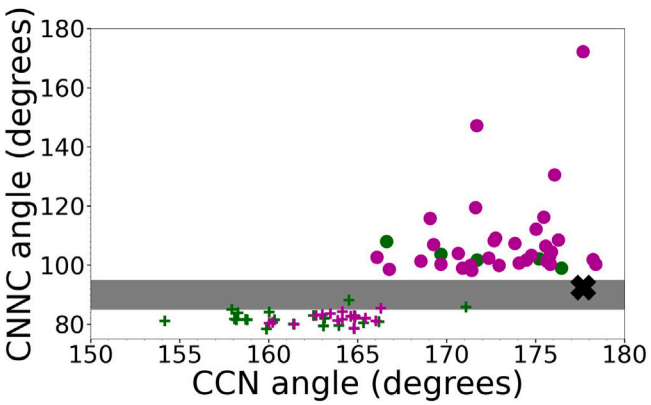


**Fig. 4.** Jumping geometries of the cis-to-trans (+) and trans-to-cis (dots) trajectories. Reactive trajectories are shown as green, while non-reactive are shown in magenta. The average optimized CI structure is shown as a black X. The grey area shows the region in which the CNNC angle is too close to the CI structure for optimized structures to be obtained. It is the same region as shown in Fig. 1a.

## 4. Cis-to-trans isomerization

### 4.1. QY and lag time

For the cis-to-trans isomerization, the calculation yielded 21 reactive (see Fig. 6) and 16 non-reactive (see Fig. 5) trajectories. Thus,

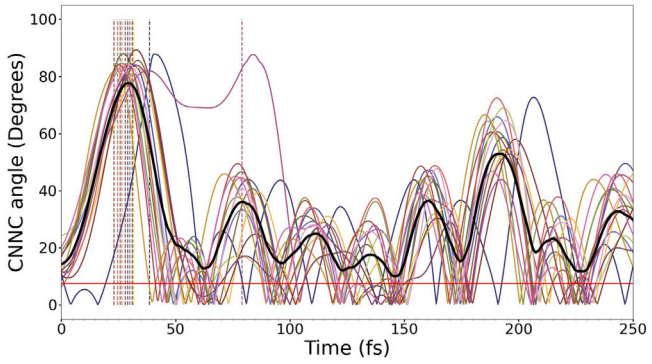


**Fig. 5.** All non-reactive trajectories from cis Azobenzene illustrated by the evolution of the dihedral angle over time. Time of jump is indicated by the vertical lines. Each colour represents one trajectory. The thick black line represents the average trajectory, while the horizontal red line shows the value of the CNNC dihedral angle of the minimum potential energy GS structure of the cis-isomer. Note that the values of the CNNC dihedral angle along the trajectories are reported only in the interval 0–180° (due to symmetry) and, therefore, that the average trajectory eventually oscillates around a larger positive value for the CNNC dihedral angle instead of the GS equilibrium value of the cis isomer.

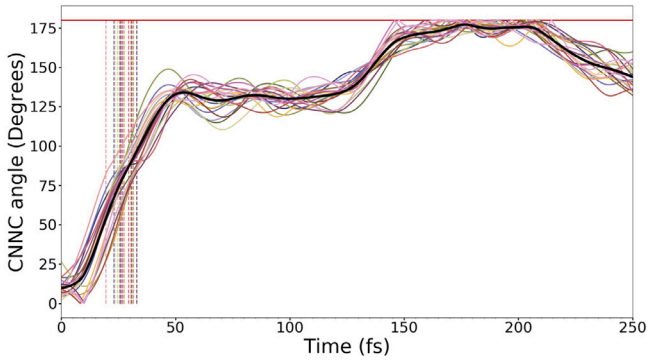


**Fig. 6.** All reactive trajectories from cis Azobenzene illustrated by the evolution of the absolute value of the dihedral angle over time. Time of jump is indicated by the vertical lines. Each colour represents one trajectory. The thick black line represents the average trajectory, while the horizontal red line shows the value of the CNNC dihedral angle at the minimum potential energy GS structure of the trans-isomer. Note that the values of the CNNC dihedral angle along the trajectories are reported only in the interval 0–180° (due to symmetry) and, therefore, that the average trajectory always stays at a value for the CNNC dihedral angle below 180°.

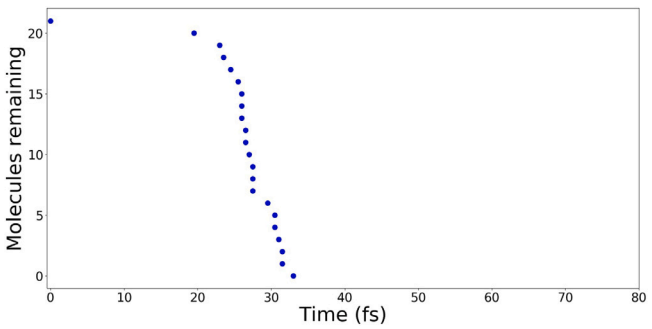


**Fig. 7.** Time of jump for all reactive trajectories. Each point signifies the jumping time of one reactive trajectory. Observe that the point at $t = 0.0$ has been added.

a QY of 57% was obtained in good agreement with previous calculations (10%-63% [4], 34%-65% [3] and 45%-68% [6]) and experiment (41%–56%) [2].

The time of jump for reactive trajectories was also considered (see Fig. 7) and found to be 19.5 fs–33 fs, yielding a lag time of 27.33 fs, in reasonably good agreement with previously calculated lifetimes using the TDDFT method (52.7 fs–63.1 fs [3] and 33.9–63 fs [4]) and CAS-methods (53.1 fs–67 fs [3] and 60–67 [6]), but significantly smaller than the experimental value (100–170 fs) [2]. The lag time predicted from an S-curve and the lifetime of an exponential decay are assumed to be comparable as both should give an indication of the time it takes half the molecules to jump. The shorter lag of our calculation can partly be attributed to the method as can be seen from lifetimes of approximately 35 fs being obtained for similar calculations [4]. Also, the TDDFT ES-PES [4] seems to be a little more steep going from the cis-geometry to the CI compared to the ES-PES calculated using CASSCF [5,6]. Another factor, that will shorten the lag time compared to experimental and CASSCF lifetimes is the forcing of the jump. It should also be emphasized that our calculation shows ballistic dynamics rather than exponential, which might also be the cause of the discrepancy with the experimental lifetime. We do however note that such non-exponential decays are not only observed in TDDFT calculations but also in CASSCF simulations [6].

Hence, the simulation is deemed to describe the dynamics of the reaction to a satisfactory degree.

### 4.2. Normal mode analysis

It can be observed from Fig. 6 that while the jump to the trans GS happens after approximately 25 fs, it is only after 150 fs that the trajectories reach the equilibrium value of the dihedral angle for the trans-isomer. Indeed it seems the dihedral angle settles around a value of approximately 130° for about 100 fs. This feature is also observable in other TDDFT studies [3,9,10] and a recently published SA-CASSCF study [34], however it is not further investigated in either of these studies. Thus, it would appear that there might be other degrees of freedom at play than the CNNC dihedral angle traditionally investigated, as also mentioned by Böckmann et al. [9–11].

Rather than investigating certain DOFs related to important atoms or relevant for a certain mechanism, we now investigate which of all the DOFs are the most dominant. This is done by performing a normal mode analysis. As the molecule before the jump resembles the cis-isomer the most, the first 25 fs of the reaction were considered in relation to the normal modes of this isomer. Likewise, during the latter part of the reaction starting from 50 fs (were the CNNC dihedral angle is above 90° and the molecule thus can be considered to move on the trans-isomer GS) the molecule resembles the trans-isomer. Hence, this part of the reaction was considered in relation to the trans-isomer normal modes.

By visualizing the activity of the relevant normal modes (see SI for movies of trans-isomer normal modes 2 and 5), Fig. 8 was obtained. From here it can be seen that the most active modes during the first 25 fs of the reaction are modes 1–3. The remaining modes are however, also quite active, and thus while the first three normal modes might give a good indication of the important geometrical parameters, they are not expected to fully describe the dynamics on the ES. Considering instead the time following the jump and until the trans-isomer equilibrium structure is reached, it is clear that two trans-isomer normal modes 2 and 5 are significantly more active than the rest. Indeed, the remaining normal modes seem to show very little activity. Hence, these two normal modes are expected to be good DOFs along which to describe the reaction at least after the jump to the GS. Modes 2 and 5 can be related to the CNNC dihedral angle and the CCN angle as can be seen in Section 4.3. For further analysis of modes 2 and 5, see also the SI, section 2.2.2. That the reaction is well described by these two modes can also be seen in Fig. 9, where a smooth path towards the energy minimum is observed for the trajectory. The path does not appear to be the steepest possible downhill path, however this is hardly surprising considering the large kinetic energy available to the trajectories following the jump. The oscillations of the modes at longer timescales, caused by the kinetic energy available to the

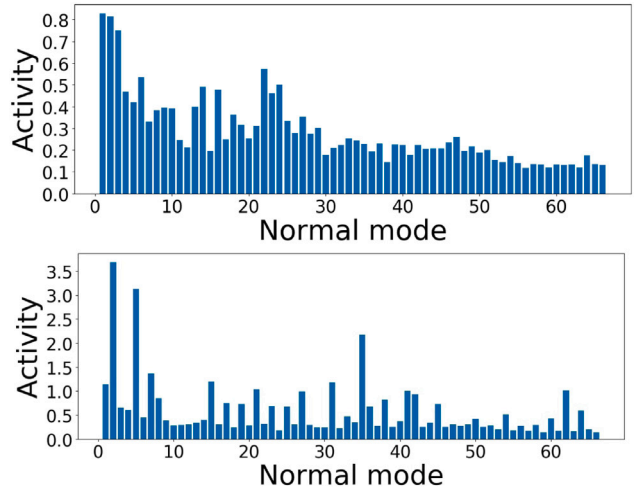


**Fig. 8.** The normal mode activity of reactive trajectories (top) between 0 fs and 25 fs for each of the cis-isomer normal modes and (bottom) between 50 fs and 150 fs for each of the trans-isomer normal modes.

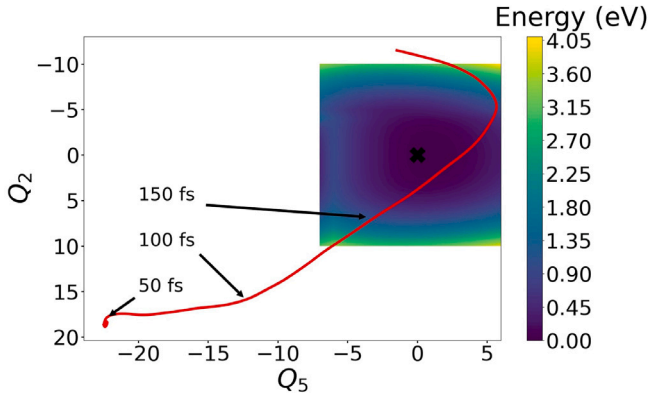


**Fig. 9.** Plot of a reactive trajectory along the trans-isomer normal modes 2 and 5. Normal mode 2 can be considered as oscillations in the CNNC and to some extent also the CCN angles, while normal mode 5 only shows oscillations in the CCN angles. The large black X marks the equilibrium structure and around this point the unrelaxed 2D-GS-PES is shown in an area, in which this unrelaxed calculation can be expected to give a reasonable description of the PES. The three black arrows show the time at the indicated points.

molecule, are evident from the top right corner of the figure, where the trajectory appears to begin to move uphill in potential energy. Observe that the unrelaxed 2D GS-PES in Fig. 9 is only meaningful close to the minimum, and hence only a small part is shown to indicate the position of this minimum. At larger displacements along only these normal modes, the structure becomes highly distorted, which allows very large (unphysical) potential energies to be reached. This indicates that relaxation to some extent does of course occur in many degrees of freedom and not solely along the two considered here.

### 4.3. Relating the normal modes to angles

Based on visualizations of relevant normal modes, as well as reactive trajectories, structural parameters were determined for further investigation. The equilibrium structure of the appropriate isomer was then displaced along one of the normal modes of interest in 10 steps in either direction (+/−). For each resulting structure the structural parameters of interest were determined. It could thus be determined which parameters were affected by the given normal mode.

Visualizing the relevant cis-isomer modes shows that they all correspond to different twisting of the benzene rings. If their effect on structural parameters as those presented in Table 1 are determined, it turns out, that only mode 3, which appears to be the least active of the three, changes the CNNC angle, while all three modes to some extent affects the CCN angle. This might be an indication, that the CCN angle should be considered, when investigating the cis-to-trans isomerization. However, as the activity plot in Fig. 8 (top) shows that practically all cis-modes to some extent are active prior to the jump, this needs to be investigated further. By considering the trans-isomer modes in Fig. 8 (bottom), very few modes are observed to be active after the jump. It is found, that the trans-isomer mode 2 is simply an out of plane bend of the CNNC angle, while the trans-isomer mode 5 is more of an in plane twist of the benzene rings. Both modes are observed to change the CCN angle, albeit the change is very small in mode 2. Only mode 2 changes the CNNC angle. Firstly, it can be observed from Fig. 10 that the CCN angles rather surprisingly decrease during the first approximately 50 fs, despite the optimized geometries for both isomers as well as the CI indicating that no change should be observed in this angle. Considering the most active cis-isomer normal modes before the jump however, they all give rise to a change in this angle, explaining this initial behaviour. Thus, our findings show that simply considering optimized geometries along the reaction path is not sufficient, when attempting to describe the full dynamics.

After the first 50 fs, the CCN angles are observed to increase from approximately 140° to 180° during the time, where the dihedral angle seems settled around 130°.

Considering mode 5 in more detail, its frequency is found to correspond to an oscillation period of approximately 150 fs corresponding well with the timescale on which the CCN angle oscillates, underlining the importance of these angles. Hence, the settling of the CNNC angle at a value below the equilibrium value as observed in Fig. 6 is ascribed to the distortion of the CCN angles, which must be relaxed sufficiently, before the CNNC angle can reach its equilibrium. As both the trans-isomer mode 2 and cis-isomer mode 3 appear to change both the CNNC and the CCN angles these DOFs must be considered coupled. Hence, once the reaction starts the cis-normal mode 3 is activated, which changes both the CNNC dihedral angle *and* distorts the CCN angle. After the jump to the trans-isomer ground state, the distortion along normal modes related to these angles, i.e. trans-isomer modes 2 and 5, will be very large causing a significant gradient and thus movement along these modes. As the displacement along normal mode 5 is larger than along mode 2, the initial movement after the jump will primarily be along this mode, thus hindering the motion along the mode related to the CNNC dihedral angle (normal mode 2), until the distortion along the two modes becomes comparable.

As what appears to be the most relevant normal modes, are strongly related to the CNNC dihedral angle and the CCN angles, it would be natural to attempt to describe the reaction along those two DOFs instead. If we simply consider the trajectories along these two angles, we obtain Fig. 11. From this figure it is evident that all trajectories behave in the same way along these two degrees of freedom, and any trajectory can thus be considered representative for the reaction. We thus investigate how a reactive trajectory moves superimposed on a relaxed GS-PES computed along the CCN and CNNC angles in Fig. 12. Firstly, it is noted from Fig. 12 that the differences in potential energies of the reactive trajectory at the points indicated by arrows are significantly larger than what would be expected from the underlying relaxed GS-PES. The GS-PES indicates a change of at most 0.5 eV, while a change of more than 1 eV is observed between the two arrows in the middle. This indicates that the relaxed GS-PES in these two degrees of freedom is not sufficient to explain the behaviour of the trajectories. In addition it is observed that, on this GS-PES, the initial movement of the trajectories are not along the steepest downhill slope towards the equilibrium structure. In fact, the trajectory appears to move with roughly constant potential energy. To investigate if this is caused by a potential energy barrier, a trajectory was simulated from the structure directly following the forced jump with zero initial

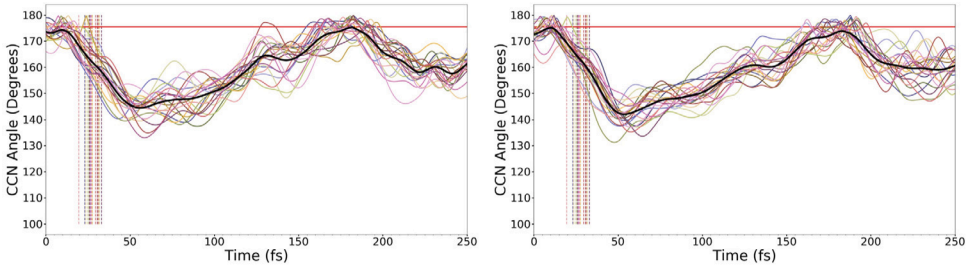


(a) Evolution of the CCN angle (b) Evolution of the NCC angle

**Fig. 10.** All reactive trajectories from cis Azobenzene illustrated by CCN (10a) and NCC (10b) angles between the two carbons at the ends of the benzene ring and the closest nitrogen of the azo-group over time. Time of jump is indicated by the vertical lines. Each colour represents one trajectory, while the thick black line represents the average trajectory. The horizontal red line shows the value of the CCN angle at the minimum potential energy GS trans-isomer structure.

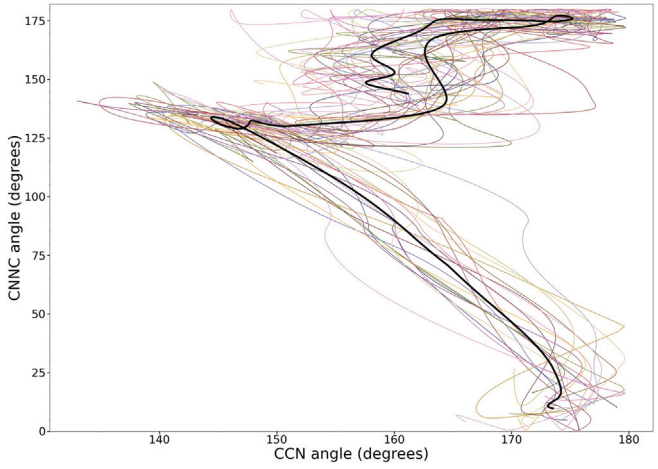


**Fig. 11.** Evolution of the CNNC angle vs the CCN angle of all reactive trajectories. Each colour represents one trajectory. The thick black line represents the average trajectory.

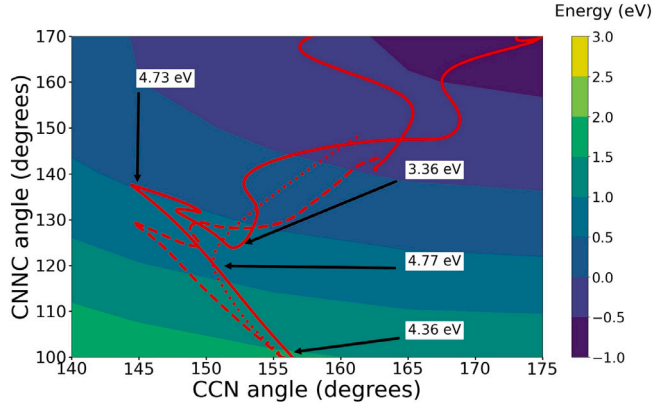


**Fig. 12.** 2D relaxed GS-PES along CNNC dihedral angle and the CCN angle (the corresponding NCC angle has been allowed to relax) overlaid with reactive cis-to-trans trajectories. The energies of the trajectory is observed to be much higher than those of the underlying PES, indicating a highly distorted molecular structure and hence, that the reaction cannot simply be considered along the CNNC and CCN angles, while all other DOFs relax. The black arrows show the potential energy of the reactive trajectory (solid red line) at the points indicated. The corresponding MEP (dotted red line) and trajectories starting with zero velocity (dashed red line) from the structure of the reactive trajectory directly following the forced jump to the GS is also shown.

velocity. This trajectory however is found to move in the same way as the original trajectory and thus it appears that it is not an energy barrier at this point that hinders the most direct movement towards the equilibrium structure. A minimum energy path (MEP) was also

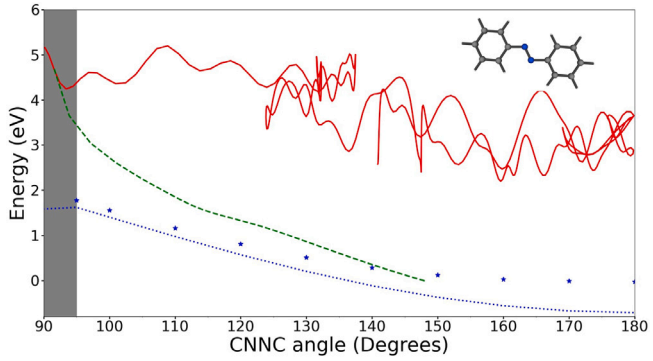


**Fig. 13.** Potential energy vs. CNNC angle on the trans-isomer side of the 1D-PES. The potential energy found by a relaxed energy scan is shown in blue for the GS (dotted) and for the GS potential energies computed from relaxed ES structures (stars). The green line represents the MEP of a (representative) reactive trajectory starting from the structure obtained shortly after the jump to the GS. The red line shows the actual potential energy of that same trajectory during simulation as also shown in Fig. 12. The potential energy equal to zero here corresponds to the energy of the equilibrium structure of the cis-isomer in the GS.

computed on the full-dimensional GS-PES from the structure directly following the forced jump and evidently shows the same movement trends in the CCN and CNNC angles as the other trajectories plotted. However, the MEP is observed to be significantly smoother than the trajectories that allow kinetic energy to be picked up along the path, which would allow for movement also towards areas of larger potential energy.

The observed behaviour indicates that the molecule needs to rearrange most likely due to a significant strain along these DOFs, before the equilibrium structure can be reached. This finding is in good agreement with the previously proposed twist mechanism [9,10], which does indeed consist in a change of the CNNC dihedral angle followed by rearrangement of the benzene rings. To investigate this further, the 1D relaxed GS-PES along the CNNC angle is considered. From Fig. 13 it is evident that the potential energy of the MEP and actual trajectory is initially much higher than for the relaxed structures. This however can be explained by the starting point of the calculation, which is a highly distorted structure compared to the 2D relaxed GS-PES. The main point of interest to note however, is that the slope of the MEP curve is much steeper than any of the relaxed curves indicating other degrees of freedom at play. This can also be seen from the actual trajectory, which shows an initial drop in potential energy, only to then use the gained kinetic energy to move towards an area of higher potential energy. This gain in kinetic energy also explains the many twists of the trajectory on the 2D relaxed GS-PES and indeed from Fig. 12 the MEP is observed to move rather smoothly towards the minimum potential energy point after the initial detour. This detour however cannot be

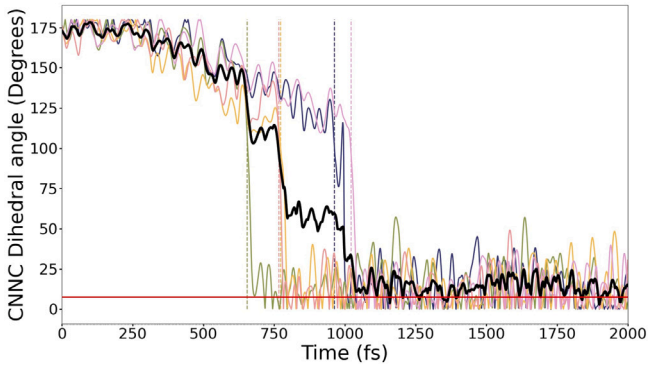


**Fig. 14.** Time evolution of the CNNC dihedral angle of all reactive trajectories starting from trans-azobenzene. Vertical lines indicate jump times.Each colour represents one trajectory. The horizontal red line shows the value of the CNNC dihedral angle at the minimum potential energy GS structure of the cis-isomer. The thick black curve shows the average reactive trajectory. Note that the values of the CNNC dihedral angle along the trajectories are reported only in the interval 0–180° (due to symmetry) and, therefore, that the average trajectory eventually oscillates around a larger positive value for the CNNC dihedral angle instead of the GS equilibrium value of the cis isomer.

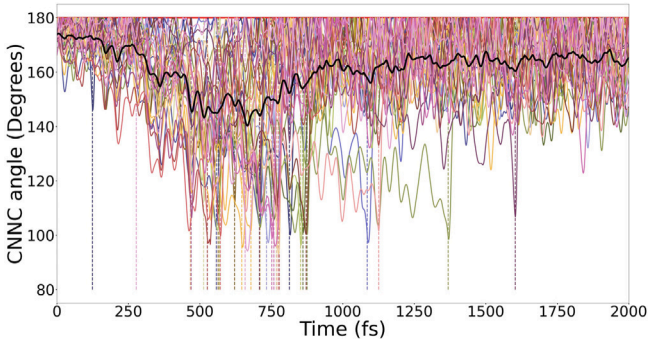


**Fig. 15.** Time evolution of the CNNC dihedral angle of all non-reactive trajectories starting from trans-azobenzene. Vertical lines indicate jump times. Each colour represents one trajectory. The horizontal red line shows the value of the CNNC dihedral angle at the minimum potential energy GS structure of the trans-isomer. The thick black curve shows the average non-reactive trajectory. Note that the values of the CNNC dihedral angle along the trajectories are reported only in the interval 0–180° (due to symmetry) and, therefore, that the average trajectory always stays at a value for the CNNC dihedral angle below 180°.

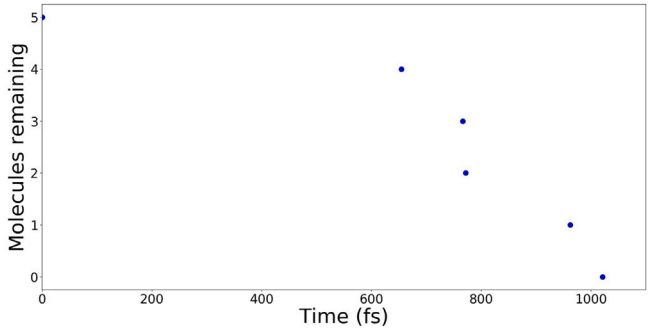


**Fig. 16.** Plot of jump times of the trans-to-cis isomerization. Each point represents the jump time of one reactive trajectory. Observe that the point at $t = 0.0$ has been added.

explained by the 1D relaxed GS-PES. While the MEP does not move uphill in potential energy on the 2D relaxed GS-PES, it does not take the most direct route towards the minimum, indicating that while the two angles provide a good description of the reaction, they do not provide as full a picture of the reaction after the time of jump as the two trans-isomer normal modes. In addition, allowing the remaining DOFs to relax, while changing the CNNC and CCN angles was shown in Fig. 12 to produce a wrong description of the process, and thus we cannot study this reaction by a few static electronic structure calculations, but rather we need to simulate the actual dynamics in order to explain the isomerization, since the molecule during reaction appears to be very far from relaxed.

## 5. Trans-to-cis isomerization

### 5.1. QY and lag time

We now turn our attention to the slower trans-to-cis isomerization. From Fig. 1 a significantly lower QY of the trans-to-cis isomerization compared to that of the cis-to-trans isomerization was anticipated. Indeed, of the 38 simulated trajectories, 33 were non-reactive (See Fig. 15 and for further details section 3.2 in the SI), while 5 were reactive (See Fig. 14). This gives a QY of approximately 13.2%, which is in reasonable agreement with experiment (23%–35%) [2] and other simulations (11%–33%) [3] although on the low side.

Considering the jump times of the trans-to-cis reaction (0.655 ps–1.02 ps), a lag time of 0.84 ps is obtained (See Fig. 16), in good agreement with the experimental lifetime (0.9 ps–1.4 ps) [2]. This comparison has already been justified above. That the lag time is shorter than the experimentally determined lifetime is expected as the jump is forced.

In addition to the reasonable agreement with experiment, we observe that the reactive trajectories are very consistent in their behaviour. Hence, despite the small number of trajectories investigated, the simulation can be expected to offer a representative description of the reactive reaction path, thus allowing us to gain insights into the dynamics.

The non-reactive trajectories are observed to behave less consistently than the reactive ones with respect to the value of the CNNC angle at the time of jump. Here, a wide range of different values are observed, as can be seen from Fig. 15. As the non-reactive trajectories are not the main point of interest here, this will not be investigated or discussed further.

### 5.2. Explaining the longer timescale

In order to investigate the reason for the long lifetime of the trans-to-cis isomerization one might investigate the evolution of the often reported CNN angles over time, however as seen in Fig. 13 of the SI, no obvious indication of the relaxation of the CNN angles being a driving force can be seen.

Observing closely the evolution of the CNNC dihedral angle of the reactive trajectories in Fig. 14 prior to the jump to the ground state one can see a fairly smooth decrease in the CNNC dihedral angle over time. Indeed, if one considers an average reactive trajectory before the jump, one can fit a cosine function to this average, as seen in Fig. 17. The fit is reasonable good and would correspond to an ES oscillation half-period from the trans- (180°) to the cis-isomer (ca. 0°) of approximately 2.4 ps. A quarter period (1.2 ps) thus corresponds to the reaction time, i.e. the time it takes to reach the CI at a CNNC dihedral angle of approximately 90°. This reaction time is in good agreement with the experimentally determined lifetime of the reaction (0.9 ps–1.4 ps) [2]. The smoothness of the curve prior to the jump indicates that no potential energy barrier is present during the simulation as also expected from the 1D-ES-PES in Fig. 1a, when the forced jump is taken into account, and thus this cannot be the cause of the longer timescale. In addition, the good agreement between the oscillation period of the fitted cosine curve and the experimental lifetime indicates that the longer timescale of the trans-to-cis isomerization is simply a result of a slow (quarter of an) oscillation of the CNNC dihedral angle in the ES.

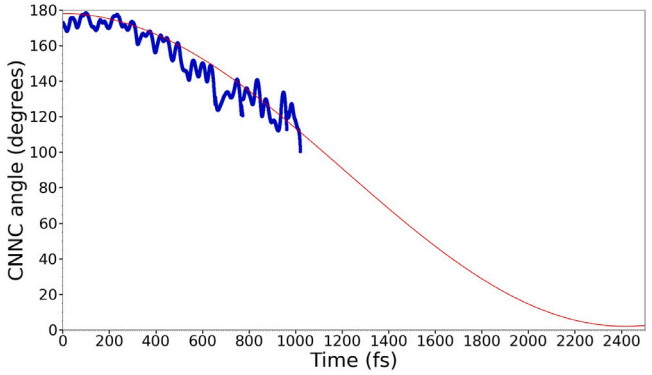


**Fig. 17.** Time evolution of the CNNC dihedral angle of an average of the reactive trans-to-cis trajectories (blue curve) fitted to a cosine function, $\theta_{CNNC} = 90° + 88° \cos\left(\frac{2\pi}{4833\ \text{fs}} \cdot t\right)$ (red curve). The evolution of the fit up to the point where a dihedral angle of approximately zero degrees (cis-isomer) is shown.

## 6. Conclusion

Simulations of the isomerization of Azobenzene have been carried out utilizing the procedure of forced jumps within the surface hopping framework in order to circumvent the problems often arising for TDDFT calculations around the area of the CI between the GS and first excited state.

The simulations for both the cis-to-trans and trans-to-cis isomerization showed results of QY and lag times in reasonable agreement with previous studies and experiment. In addition, the trajectories of the same type all seemed to behave in the same way with the exception of the non-reactive trans-to-cis trajectories, which showed a wider range of jumping values for the CNNC angle. It has therefore been concluded that the investigated reactive trajectories give a sufficiently representative description of the structural evolution of the molecule during the photoisomerization.

It was found that the cis-to-trans isomerization occurs as a result of movement along two normal modes, rather than simply along the CNNC dihedral angle, which is the most common description. While the first normal mode is largely responsible for the change in the dihedral angle both modes also influence the CCN angle between the benzene ring and the azobond, and the change in this angle appears to halt the change in the dihedral angle. It was found that while these two angles seem to be the most important in the reaction other degrees of freedom might also be needed in describing the reaction in such a coordinate system, as the description here did not appear as adequate as the one offered by considering the reaction along the two normal modes. Our observations for the cis-to-trans isomerization corroborate the previously proposed two-step twist mechanism. In contrast to the cis-to-trans isomerization, the trans-to-cis isomerization seems to happen in one smooth step albeit a slow one. The isomerization appears to simply be a result of slow excited-state oscillations in the CNNC dihedral angle, without the impediment of a significant potential energy barrier.

Finally, the importance of the previously reported planar CI was investigated and, while more studies will be required, it appears that the significance of this CI is not only geometry dependent as suggested in other studies, but is also strongly influenced by the choice of functional.

## CRediT authorship contribution statement

**Anna Kristina Schnack-Petersen:** Writing – review & editing, Writing – original draft, Investigation, Formal analysis, Data curation, Visualization. **Mátyás Pápai:** Conceptualization, Formal analysis, Funding acquisition, Investigation, Supervision, Writing – review & editing. **Klaus Braagaard Møller:** Writing – review & editing, Supervision, Investigation, Funding acquisition, Formal analysis, Conceptualization.

## Declaration of competing interest

The authors declare that they have no known competing financial interests or personal relationships that could have appeared to influence the work reported in this paper.

## Acknowledgements

The research leading to the presented results has received funding from the Hungarian National Research, Development and Innovation Fund, Grant No. NKFIH PD 134976 (MP), the Government of Hungary and the European Regional Development Fund under grant VEKOP-2.3.2-16-2017-00015 (MP), and the Independent Research Fund Denmark, Grant No. 8021-00347B (KBM,MP).

MP acknowledges support from the János Bolyai Scholarship of the Hungarian Academy of Sciences.

AKSP thanks the DTU Partnership PhD programme for funding.

## Appendix A. Supplementary data

Supplementary material related to this article can be found online at https://doi.org/10.1016/j.jphotochem.2022.113869.

- Further computational details
- Evaluation of a suitable potential energy gap for the forced jump
- Tables reporting jumping geometries
- Tables reporting optimized CI geometries
- Further investigations of the potential energy evoultion of the cis-to-trans isomerization
- Additional normal mode analysis of trans-isomer normal modes
- Results for the cis-to-trans isomerization using the B3LYP functional
- Investigation of non-reactive trans-to-cis trajectories
- Investigation of the evolution of the CNN angles for reactive trans-to-cis trajectories
- Results for the trans-to-cis isomerization using the B3LYP functional
- Movies of BHHLYP cis-isomer normal modes 1–3
- Movies of BHHLYP trans-isomer normal modes 2 and 5
- Movies of 2 BHHLYP non-reactive and 2 reactive cis-to-trans trajectories
- Movies of 2 BHHLYP non-reactive and 2 reactive trans-to-cis trajectories

## References

[1] G. Hartley, The cis-form of azobenzene, Nature 140 (1937) 281, http://dx.doi.org/10.1038/140281a0.

[2] H.M. Bandara, S.C. Burdette, Photoisomerization in different classes of azobenzene, Chem. Soc. Rev. 41 (5) (2012) 1809–1825, http://dx.doi.org/10.1039/c1cs15179g.

[3] L. Yue, Y. Liu, C. Zhu, Performance of tddft with and without spin-flip in trajectory surface hopping dynamics: cis–trans azobenzene photoisomerization, Phys. Chem. Chem. Phys. 20 (2018) 24123–24139, http://dx.doi.org/10.1039/C8CP03851A.

[4] L. Ye, C. Xu, F.L. Gu, C. Zhu, Functional and basis set dependence for time-dependent density functional theory trajectory surface hopping molecular dynamics: Cis-azobenzene photoisomerization, J. Comput. Chem. 41 (7) (2020) 635–645, http://dx.doi.org/10.1002/jcc.26116, arXiv:https://onlinelibrary.wiley.com/doi/pdf/10.1002/jcc.26116. URL https://onlinelibrary.wiley.com/doi/abs/10.1002/jcc.26116.

[5] J. Casellas, M.J. Bearpark, M. Reguero, Excited-state decay in the photoisomerisation of azobenzene: A new balance between mechanisms, Chem. Phys. Chem. 17 (19) (2016) 3068–3079, http://dx.doi.org/10.1002/cphc.201600502, arXiv:https://chemistry-europe.onlinelibrary.wiley.com/doi/pdf/10.1002/cphc.201600502. URL https://chemistry-europe.onlinelibrary.wiley.com/doi/abs/10.1002/cphc.201600502.

[6] M. Pederzoli, J. Pittner, M. Barbatti, H. Lischka, Nonadiabatic molecular dynamics study of the cis–trans photoisomerization of azobenzene excited to the s1 state, J. Phys. Chem. A 115 (41) (2011) 11136–11143, http://dx.doi.org/10.1021/jp2013094, arXiv:https://doi.org/10.1021/jp2013094.

[7] G. Granucci, M. Persico, Excited state dynamics with the direct trajectory surface hopping method: azobenzene and its derivatives as a case study, Theor. Chem. Acc. 117 (2007) 1131–1143, http://dx.doi.org/10.1007/s00214-006-0222-1.

[8] E. Wei-Guang Diau, A new trans-to-cis photoisomerization mechanism of azobenzene on the s1(n, $\pi^*$) surface, J. Phys. Chem. A 108 (6) (2004) 950–956, http://dx.doi.org/10.1021/jp031149a, arXiv:https://doi.org/10.1021/jp031149a.

[9] M. Böckmann, N.L. Doltsinis, D. Marx, Azobenzene photoswitches in bulk materials, Phys. Rev. E 78 (2008) 036101, http://dx.doi.org/10.1103/PhysRevE.78.036101, URL https://link.aps.org/doi/10.1103/PhysRevE.78.036101.

[10] M. Böckmann, N.L. Doltsinis, D. Marx, Nonadiabatic hybrid quantum and molecular mechanic simulations of azobenzene photoswitching in bulk liquid environment, J. Phys. Chem. A 114 (2) (2010) 745–754, http://dx.doi.org/10.1021/jp910103b, arXiv:https://doi.org/10.1021/jp910103b.

[11] M. Böckmann, S. Braun, N.L. Doltsinis, D. Marx, Mimicking photoisomerisation of azo-materials by a force field switch derived from nonadiabatic ab initio simulations: Application to photoswitchable helical foldamers in solution, J. Chem. Phys. 139 (8) (2013) 084108, http://dx.doi.org/10.1063/1.4818489, arXiv:https://doi.org/10.1063/1.4818489.

[12] J.A. Gámez, O. Weingart, A. Koslowski, W. Thiel, Cooperating dinitrogen and phenyl rotations in trans-azobenzene photoisomerization, J. Chem. Theory Comput. 8 (7) (2012) 2352–2358, http://dx.doi.org/10.1021/ct300303s, pMID: 26588968. arXiv:https://doi.org/10.1021/ct300303s.

[13] Z. Mahimwalla, J. Yager, K.G. Mamiya, A. Shishido, A. Priimagi, C.J. Barret, Azobenzene photomechanics: prospects and potential applications, Polym. Bull. 69 (2012) 967–1006, http://dx.doi.org/10.1007/s00289-012-0792-0.

[14] J. García-Amorós, D. Velasco, Recent advances towards azobenzene-based light-driven real-time information-transmitting materials, Beilstein J. Org. Chem. 8 (2012) 1003–1017, http://dx.doi.org/10.3762/bjoc.8.113.

[15] N. Tamai, H. Miyasaka, Ultrafast dynamics of photochromic systems, Chem. Rev. 100 (5) (2000) 1875–1890, http://dx.doi.org/10.1021/cr9800816, arXiv:https://doi.org/10.1021/cr9800816.

[16] H. Bach, K. Anderle, T. Fuhrmann, J.H. Wendorff, Biphoton-induced refractive index change in 4-amino-4'-nitroazobenzene/polycarbonate, J. Phys. Chem. 100 (10) (1996) 4135–4140, http://dx.doi.org/10.1021/jp952094i, arXiv:https://doi.org/10.1021/jp952094i.

[17] Z. Liu, C. Zhao, M. Tang, S. Cai, Electrochemistry of cis-azobenzen chromophore in coulombically linked self-assembled monolayer-langmuir–blodgett composite monolayers, J. Phys. Chem. 100 (43) (1996) 17337–17344, http://dx.doi.org/10.1021/jp9536615, arXiv:https://doi.org/10.1021/jp9536615.

[18] P.H. Rasmussen, P.S. Ramanujam, S. Hvilsted, R.H. Berg, A remarkably efficient azobenzene peptide for holographic information storage, J. Am. Chem. Soc. 121 (20) (1999) 4738–4743, http://dx.doi.org/10.1021/ja981402y, arXiv:https://doi.org/10.1021/ja981402y.

[19] R. Hagen, T. Bieringer, Photoaddressable polymers for optical data storage, Adv. Mater. 13 (23) (2001) 1805–1810, http://dx.doi.org/10.1002/1521-4095(200112)13:23<1805::AID-ADMA1805>3.0.CO;2-V, arXiv:https://onlinelibrary.wiley.com/doi/pdf/10.1002/1521-4095%28200112%2913%3A23%3C1805%3A%3AAID-ADMA1805%3E3.0.CO%3B2-V. URL https://onlinelibrary.wiley.com/doi/abs/10.1002/1521-4095%28200112%2913%3A23%3C1805%3A%3AAID-ADMA1805%3E3.0.CO%3B2-V.

[20] M. Abedi, M. Pápai, N.E. Henriksen, K.B. Møller, M.B. Nielsen, K.V. Mikkelsen, Theoretical investigation on the control of macrocyclic dihydroazulene/azobenzene photoswitches, J. Phys. Chem. C 123 (42) (2019) 25579–25584, http://dx.doi.org/10.1021/acs.jpcc.9b06975, arXiv:https://doi.org/10.1021/acs.jpcc.9b06975.

[21] T. Ikeda, O. Tsutsumi, Optical switching and image storage by means of azobenzene liquid-crystal films, Science 268 (5219) (1995) 1873–1875, http://dx.doi.org/10.1126/science.268.5219.1873, arXiv:https://science.sciencemag.org/content/268/5219/1873.full.pdf. URL https://science.sciencemag.org/content/268/5219/1873.

[22] J. Pang, C. Gao, L. Shu, X. Hu, M. Li, Dft calculations: Bridged-azo working with visible light, Comput. Theor. Chem. 1191 (2020) 113041, http://dx.doi.org/10.1016/j.comptc.2020.113041, URL https://www.sciencedirect.com/science/article/pii/S2210271X20303418.

[23] A. Natansohn, P. Rochon, Photoinduced motions in azo-containing polymers, Chem. Rev. 102 (11) (2002) 4139–4176, http://dx.doi.org/10.1021/cr970155y, arXiv:https://doi.org/10.1021/cr970155y.

[24] V. Shibaev, A. Bobrovsky, N. Boiko, Photoactive liquid crystalline polymer systems with light-controllable structure and optical properties, Prog. Polym. Sci. 28 (5) (2003) 729–836, http://dx.doi.org/10.1016/S0079-6700(02)00086-2, URL https://www.sciencedirect.com/science/article/pii/S0079670002000862.

[25] S. Krause, J.D. Evans, V. Bon, S. Crespi, W. Danowski, W.R. Browne, S. Ehrling, F. Walenszus, D. Wallacher, N. Grimm, et al., Cooperative light-induced breathing of soft porous crystals via azobenzene buckling, 2020, http://dx.doi.org/10.26434/chemrxiv.13286009.v1, URL https://chemrxiv.org/articles/preprint/Cooperative_Light-Induced_Breathing_of_Soft_Porous_Crystals_via_Azobenzene_Buckling/13286009/1.

[26] A. Credi, Artificial molecular motors powered by light, Aust. J. Chem. 59 (2006) 157–169, http://dx.doi.org/10.1071/CH06025.

[27] T. Hugel, N.B. Holland, A. Cattani, L. Moroder, M. Seitz, H.E. Gaub, Single-molecule optomechanical cycle, Science 296 (5570) (2002) 1103–1106, http://dx.doi.org/10.1126/science.1069856, arXiv:https://science.sciencemag.org/content/296/5570/1103.full.pdf. URL https://science.sciencemag.org/content/296/5570/1103.

[28] A. Harada, Cyclodextrin-based molecular machines, Acc. Chem. Res. 34 (6) (2001) 456–464, http://dx.doi.org/10.1021/ar000174l, arXiv:https://doi.org/10.1021/ar000174l.

[29] R. Ballardini, V. Balzani, A. Credi, M.T. Gandolfi, M. Venturi, Artificial molecular-level machines: Which energy to make them work? Acc. Chem. Res. 34 (6) (2001) 445–455, http://dx.doi.org/10.1021/ar000170g, arXiv:https://doi.org/10.1021/ar000170g.

[30] P. Tavadze, G. Avendaño Franco, P. Ren, X. Wen, Y. Li, J.P. Lewis, A machine-driven hunt for global reaction coordinates of azobenzene photoisomerization, J. Am. Chem. Soc. 140 (1) (2018) 285–290, http://dx.doi.org/10.1021/jacs.7b10030, arXiv:https://doi.org/10.1021/jacs.7b10030.

[31] F. Aleotti, L. Soprani, A. Nenov, R. Berardi, A. Arcioni, C. Zannoni, M. Garavelli, Multidimensional potential energy surfaces resolved at the raspt2 level for accurate photoinduced isomerization dynamics of azobenzene, J. Chem. Theory Comput. 15 (12) (2019) 6813–6823, http://dx.doi.org/10.1021/acs.jctc.9b00561, pMID: 31647648. arXiv:https://doi.org/10.1021/acs.jctc.9b00561.

[32] J.K. Yu, C. Bannwarth, R. Liang, E.G. Hohenstein, T.J. Martínez, Nonadiabatic dynamics simulation of the wavelength-dependent photochemistry of azobenzene excited to the n$\pi^*$ and $\pi\pi^*$ excited states, J. Am. Chem. Soc. 142 (49) (2020) 20680–20690, http://dx.doi.org/10.1021/jacs.0c09056, pMID: 33228358. arXiv:https://doi.org/10.1021/jacs.0c09056.

[33] F. Segatta, A. Nenov, S. Orlandi, A. Arcioni, S. Mukamel, M. Garavelli, Exploring the capabilities of optical pump x-ray probe nexafs spectroscopy to track photo-induced dynamics mediated by conical intersections, Faraday Discuss. 221 (2020) 245–264, http://dx.doi.org/10.1039/C9FD00073A.

[34] I.C.D. Merritt, D. Jacquemin, M. Vacher, Cis → trans photoisomerisation of azobenzene: a fresh theoretical look, Phys. Chem. Chem. Phys. 23 (2021) 19155–19165, http://dx.doi.org/10.1039/D1CP01873F.

[35] F. He, X. Ren, J. Jiang, G. Zhang, L. He, Real-time, time-dependent density functional theory study on photoinduced isomerizations of azobenzene under a light field, J. Phys. Chem. Lett. 13 (2) (2022) 427–432, pMID: 34989580. arXiv:https://doi.org/10.1021/acs.jpclett.1c03442.

[36] S. Saeed, P.A. Channar, A. Saeed, F.A. Larik, Fluorescence modulation of cdte nanowire by azobenzene photochromic switches, J. Photochem. Photobiol. A 369 (2019) 159–165, http://dx.doi.org/10.1016/j.jphotochem.2018.09.035, URL https://www.sciencedirect.com/science/article/pii/S1010603018309158.

[37] L. Yu, C. Xu, Y. Lei, C. Zhu, Z. Wen, Trajectory-based nonadiabatic molecular dynamics without calculating nonadiabatic coupling in the avoided crossing case: trans ⟷ cis photoisomerization in azobenzene, Phys. Chem. Chem. Phys. 16 (2014) 25883–25895, http://dx.doi.org/10.1039/C4CP03498H.

[38] D. Keefer, F. Aleotti, J.R. Rouxel, F. Segatta, B. Gu, A. Nenov, M. Garavelli, S. Mukamel, Imaging conical intersection dynamics during azobenzene photoisomerization by ultrafast x-ray diffraction, Proc. Natl. Acad. Sci. USA 118 (3) (2021) http://dx.doi.org/10.1073/pnas.2022037118, arXiv:https://www.pnas.org/content/118/3/e2022037118.full.pdf. URL https://www.pnas.org/content/118/3/e2022037118.

[39] K. Burke, J. Werschnik, E.K.U. Gross, Time-dependent density functional theory: Past, present, and future, J. Chem. Phys. 123 (6) (2005) 062206, http://dx.doi.org/10.1063/1.1904586, arXiv:https://doi.org/10.1063/1.1904586.

[40] D.L. Wheeler, L.E. Rainwater, A.R. Green, A.L. Tomlinson, Modeling electrochromic poly-dioxythiophene-containing materials through tddft, Phys. Chem. Chem. Phys. 19 (2017) 20251–20258, http://dx.doi.org/10.1039/C7CP04130F.

[41] W. Li, X. Cai, Y. Hu, Y. Ye, M. Luo, J. Hu, A tddft study of the low-lying excitation energies of polycyclic cinnolines and their carbocyclic analogues, J. Mol. Struct. - THEOCHEM 732 (1) (2005) 21–32, http://dx.doi.org/10.1016/j.theochem.2005.06.042, URL https://www.sciencedirect.com/science/article/pii/S0166128005005476.

[42] C.Y. Cheng, M.S. Ryley, M.J. Peach, D.J. Tozer, T. Helgaker, A.M. Teale, Molecular properties in the tamm–dancoff approximation: indirect nuclear spin–spin coupling constants, Mol. Phys. 113 (13–14) (2015) 1937–1951, http://dx.doi.org/10.1080/00268976.2015.1024182, arXiv:https://doi.org/10.1080/00268976.2015.1024182.

[43] B.G. Levine, C. Ko, J. Quenneville, T.J. Martínez, Conical intersections and double excitations in time-dependent density functional theory, Mol. Phys. 104 (5–7) (2006) 1039–1051, http://dx.doi.org/10.1080/00268970500417762, arXiv:https://doi.org/10.1080/00268970500417762.

[44] M. Abedi, M. Pápai, K.V. Mikkelsen, N.E. Henriksen, K.B. Møller, Mechanism of photoinduced dihydroazulene ring-opening reaction, J. Phys. Chem. Lett. 10 (14) (2019) 3944–3949, http://dx.doi.org/10.1021/acs.jpclett.9b01522, arXiv:https://doi.org/10.1021/acs.jpclett.9b01522.

[45] M. Pápai, X. Li, M.M. Nielsen, K.B. Møller, Trajectory surface-hopping photoinduced dynamics from rydberg states of trimethylamine, Phys. Chem. Chem. Phys. (2021) http://dx.doi.org/10.1039/D1CP00771H.

[46] M. Richter, P. Marquetand, J. González-Vázquez, I. Sola, L. González, SHARC: ab initio molecular dynamics with surface hopping in the adiabatic representation including arbitrary couplings, J. Chem. Theory Comput. 7 (5) (2011) 1253–1258, http://dx.doi.org/10.1021/ct1007394.

[47] A. Hutcheson, A.C. Paul, R.H. Myhre, H. Koch, I.-M. Høyvik, Describing ground and excited state potential energy surfaces for molecular photoswitches using coupled cluster models, J. Comput. Chem. 42 (20) (2021) 1419–1429, http://dx.doi.org/10.1002/jcc.26553, arXiv:https://onlinelibrary.wiley.com/doi/pdf/10.1002/jcc.26553. URL https://onlinelibrary.wiley.com/doi/abs/10.1002/jcc.26553.

[48] S. Mai, P. Marquetand, L. González, Nonadiabatic dynamics: The sharc approach, WIREs Comput. Mol. Sci. 8 (2018) e1370, http://dx.doi.org/10.1002/wcms.1370.

[49] S. Mai, M. Richter, M. Heindl, M.F.S.J. Menger, A. Atkins, M. Ruckenbauer, F. Plasser, L.M. Ibele, S. Kropf, M. Oppel, P. Marquetand, L. González, Sharc2.1: Surface hopping including arbitrary couplings — program package for non-adiabatic dynamics, 2019, sharc-md.org.

[50] F. Neese, The orca program system, WIREs Comput. Mol. Sci. 2 (1) (2012) 73–78, http://dx.doi.org/10.1002/wcms.81, arXiv:https://onlinelibrary.wiley.com/doi/pdf/10.1002/wcms.81. URL https://onlinelibrary.wiley.com/doi/abs/10.1002/wcms.81.

[51] F. Neese, Software update: the orca program system, version 4.0, WIREs Comput. Mol. Sci. 8 (1) (2018) e1327, http://dx.doi.org/10.1002/wcms.1327, arXiv:https://onlinelibrary.wiley.com/doi/pdf/10.1002/wcms.1327. URL https://onlinelibrary.wiley.com/doi/abs/10.1002/wcms.1327.

[52] B.G. Levine, J.D. Coe, T.J. Martínez, Optimizing conical intersections without derivative coupling vectors: Application to multistate multireference second-order perturbation theory (ms-caspt2), J. Phys. Chem. B 112 (2) (2008) 405–413, http://dx.doi.org/10.1021/jp0761618, arXiv:https://doi.org/10.1021/jp0761618.

[53] W. Humphrey, A. Dalke, K. Schulten, VMD – visual molecular dynamics, J. Mol. Graph. 14 (1996) 33–38.

[54] A. Stukowski, Visualization and analysis of atomistic simulation data with OVITO-the Open Visualization Tool, Modelling Simulation Mater. Sci. Eng. 18 (1) (2010) http://dx.doi.org/10.1088/0965-0393/18/1/015012.

[55] G. Schaftenaar, J. Noordik, Molden: a pre- and post-processing program for molecular and electronic structures, J. Comput. Aided Mol. Des. 14 (2000) 123–134, http://dx.doi.org/10.1023/A:1008193805436.

[56] A. Mostad, C. Rømming, A refinement of the crystal structure of cis-azobenzene, Acta Chem. Scand. 25 (10) (1971) 3561–3568, http://dx.doi.org/10.3891/acta.chem.sc{and}.25-3561.

[57] J.A. Bouwstra, A. Schouten, J. Kroon, Structural studies of the system *trans*-azobenzene/*trans*-stilbene. I. A reinvestigation of the disorder in the crystal structure of *trans*-azobenzene, $C_12H_10N_2$, Acta Crystallogr. C 39 (8) (1983) 1121–1123, http://dx.doi.org/10.1107/S0108270183007611.